L_1 adaptive control of end-tidal CO_2 by optimizing the muscular power for mechanically ventilated patients

Anake Pomprapa * Marian Walter * Christof Goebel ** Berno Misgeld * Steffen Leonhardt *

**Philips Chair for Medical Information Technology, RWTH Aachen University, Aachen, Germany (e-mail: pomprapa@hia.rwth-aachen.de).*
***Weinmann Geraete fuer Medizin GmbH, Hamburg, Germany*

Abstract: In this paper, a novel approach to control end-tidal CO_2 in mechanically ventilated patients is presented. Assuming a homogeneous lung model, a regulation of arterial CO_2 tension in blood can be achieved non-invasively using L_1 adaptive control with the aid of an extremum seeking method to set the proper respiratory rate. Using these integrated approaches, not only is end-tidal CO_2 regulated at the specific level, but also muscular power for breathing is optimized to comfort the muscles involved in the respiratory system. The simulation of the control algorithms show the distinctive results based on linear and nonlinear Hammerstein models of the process. These were obtained from measurement data from a human volunteer. The algorithm is applicable under pressure-controlled ventilation and provides a practical solution in various clinical situations.

Keywords: nonlinear control systems, adaptive control, biomedical systems

1. INTRODUCTION

Carbon dioxide (CO_2) is one of the by-products of metabolism in a living cell. In the human's respiratory system, the produced CO_2 is transported through blood circulation and is removed by the lung to the air during expiration. End-tidal CO_2 ($etCO_2$) is defined as the CO_2 pressure (in mmHg) at the end of expiration. If a homogenous lung is assumed with no pulmonary disease, $etCO_2$ can be used to estimate CO_2 partial pressure in arterial blood (P_aCO_2) at steady state (Benallal and Busso, 2000). Therefore, the control of $etCO_2$ yields a regulation of P_aCO_2 and pH balance in blood. By keeping its value in the normal range, the avoidance of hypercapnia or hypocapnia can be non-invasively achieved for patients undergoing mechanical ventilation procedures. The application of closed-loop ventilation can be used in various clinical situations, for example intensive medicine, anaesthesia, and ventilation support during sleep.

In order to comfort the muscles involved in the respiratory system, the extremum seeking method is primarily applied to minimize the power of breathing, so that the optimal respiratory rate (RR) is determined (Otis *et al.*, 1950). The patient model is subsequently identified using linear and nonlinear Hammerstein models for the evaluation of the model structure and model parameters. The simplified single-input single-output (SISO) model is used for a control system design in this complex patient-in-the-loop system. It is quite obvious that we are dealing with a nonlinear time-varying system (Pomprapa *et al.*, 2013). It is therefore straightforward using an adaptive controller for this system, where challenges for feedback control are the nonlinear, time-varying system with uncertainties depending on patient age, size, and lung condition.

Adaptive control has drawn the attention from many researchers because it requires less a priori knowledge about the bounds of the uncertain system (Feng and Lozano, 1999). Its principle is to adapt the control law to cope with the time-varying system. The foundation is based on parameter estimation and guaranteed stability in order to synthesize a control law for the converged and bounded results. Many adaptive control schemes have been developed, namely model reference adaptive control (MRAC), self tuning regulator, extremum seeking control, iterative learning control, gain scheduling or L_1 adaptive control. The aim of this article is to present a control system design for end-tidal carbon dioxide ($etCO_2$) in mechanically ventilated patients using the state-of-the-art L_1 adaptive control with output feedback.

L_1 adaptive control has successfully been applied in flight control for NASA AirSTAR aircraft (Gregory *et al.*, 2009), in a flight simulator for the SIMONA 6DOF motion-based control (Stroosma *et al.*, 2011), or in biomedical systems for anaesthesia control (Ralph *et al.*, 2011 and Kharisov *et al.*, 2012). The structure of a L_1 adaptive controller is similar to MRAC but it contains an additional low-pass filter. The mathematical proof of the L_1 adaptive controller (Hovakimyan *et al.*, 2011) clearly demonstrates that the error norm is inversely proportional to the square root of the adaptation gain. By introducing the high adaptation gain, asymptotic tracking can be achieved (Cao and Hovakimyan, 2007b). The key feature of this methodology is to guarantee L_∞ -norms bounded transient response for the errors in model states and the control signals. A low-pass filter is used to get rid of the undesired high frequencies in the control signals and the bandwidth of this filter is determined by using the L_1 small gain theorem (Cao and Hovakimyan, 2006) to stabilize the whole system.

The subsequent sections of this contribution are organized as follows. It starts with the physiological description in section 2 to provide the background for this particular process. System identification is introduced in section 3 for the evaluation of the model structure, followed by the problem statement (section 4). The L_1 adaptive control design is presented in section 5. A discussion follows in section 6 and the article ends with the conclusion.

2. PHYSIOLOGICAL DESCRIPTION

The complex physiological system of a patient undergoing mechanical ventilation can be simplified as a single-input single-output (SISO) system shown in Fig. 1. Minute ventilation (MV) denotes the volume given into the lung in one minute by a mechanical ventilator, which is computed by multiplying tidal volume (V_T) and respiratory rate (RR). MV is applied to the system and regarded as an input while $etCO_2$ is considered as the system output.

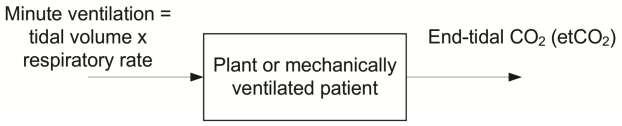

Fig. 1. SISO open-loop system for typical $etCO_2$ control.

In Fig. 2, the static nonlinearity of $etCO_2$ is presented based on an experiment with a male volunteer with a normal body mass index (BMI = 21.5 kg/m^2) at steady state. A ventilator (VENTIlogic LS, Weinmann Geraete fuer Medizin GmbH, Hamburg, Germany) was set in pressure controlled ventilation mode with a fixed positive end-expiratory pressure (PEEP) = 5 hPa and I:E ratio = 50%. Two variables i.e. peak inspiratory pressure (PIP) and RR were adjusted stepwise to change the MV. $EtCO_2$ was measured by a capnography system with integrated pulse oximetry for monitoring peripheral oxygen saturation (S_pO_2) (CO_2SMO+, Philips Respironics, Pittsburgh, USA).

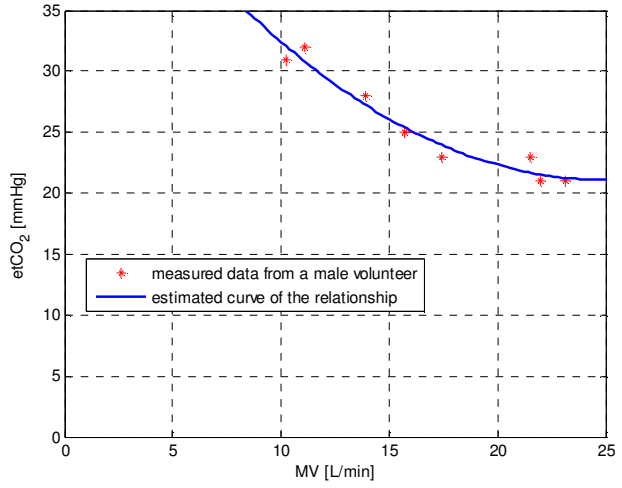

Fig. 2. Static nonlinearity between MV and $etCO_2$.

The response of $etCO_2$ shown in Fig. 2 represents a nonlinear function corresponding to the input MV. The output of the system ($etCO_2$) is inversely proportional to the input. In other words, an increment of MV leads to a decrease of $etCO_2$.

For simplification, we consider the case of a homogeneous lung model where PEEP and I:E ratio are fixed as stated. Otherwise, it would result in much more complicated modelling of multivariate inputs. Nevertheless, our simplified SISO model can be applied in real clinical practice to support or assist ventilation in intensive care or for home care.

The extremum seeking method (Tan *et al.*, 2010) is primarily carried out in order to identify the optimal RR. The computation of the power of breathing is provided in eq. (1) and is computed from every breathstroke.

$$Power = \frac{RR}{60} \cdot \int_0^{\frac{60}{RR}} P(t) \cdot \dot{V}(t) dt \qquad (1)$$

where $Power$ represents the power of one breathing (Watt), $P(t)$ symbolizes airway pressure (Nm^{-2}) and $\dot{V}(t)$ denotes airway flow (m^{3}sec^{-1}). The conversion of the units is required from hecto Pascal (hPa) to Pa or Nm^{-2} (1 hPa = 100 Pa) and from L/min to m^3/sec.

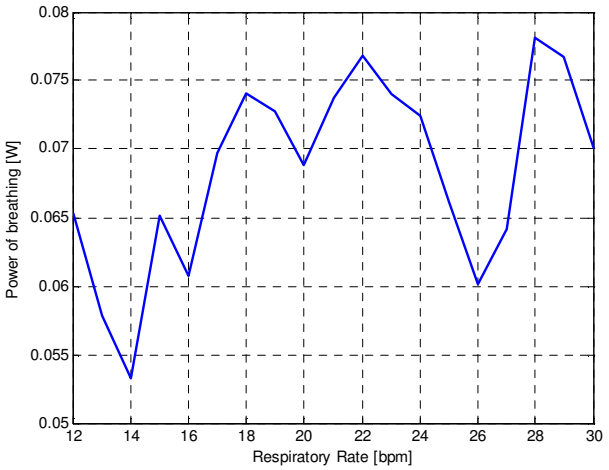

Fig. 3. A relationship between the power of breathing and respiratory rate (RR).

In Fig. 3, an initialization of the ventilation procedure is carried out to seek the optimal RR that optimizes the power of one breath cycle. By stepwise variation of RR, the power of breathing is computed and averaged for 5 consecutive breathing cycles at rest. The extremum seeking method is used to find the global minima for the power of one breathing. Based on the data from the volunteer, a RR of 14 bpm is identified and it will be used for further processes in system identification, simulation and control throughout this paper.

The formulation of the mathematical model is shifted from a consideration of MV input to pressure difference (ΔP = PIP-PEEP). Since RR is predetermined to optimize the muscular power of breathing and PEEP is also fixed, ΔP has a direct impact on the tidal volume. Therefore, ΔP is considered to be an equivalent (apart from a nonlinear gain factor) input into this system.

3. SYSTEM IDENTIFICATION

To extract the dynamics of the cardiopulmonary system, a step change of the pressure difference ($\Delta P = PIP - PEEP$) was introduced for the mechanically ventilated patient. The range of pressure difference (ΔP) was set between 2 and 10 hPa with PEEP of 5 hPa, I:E ratio of 50%, RR of 14 bpm and oxygen concentration (FiO_2) of 0.21 or 21%. Using these settings, various minute ventilation steps were given into the system and it resulted in the output end-tidal CO_2 ($etCO_2$).

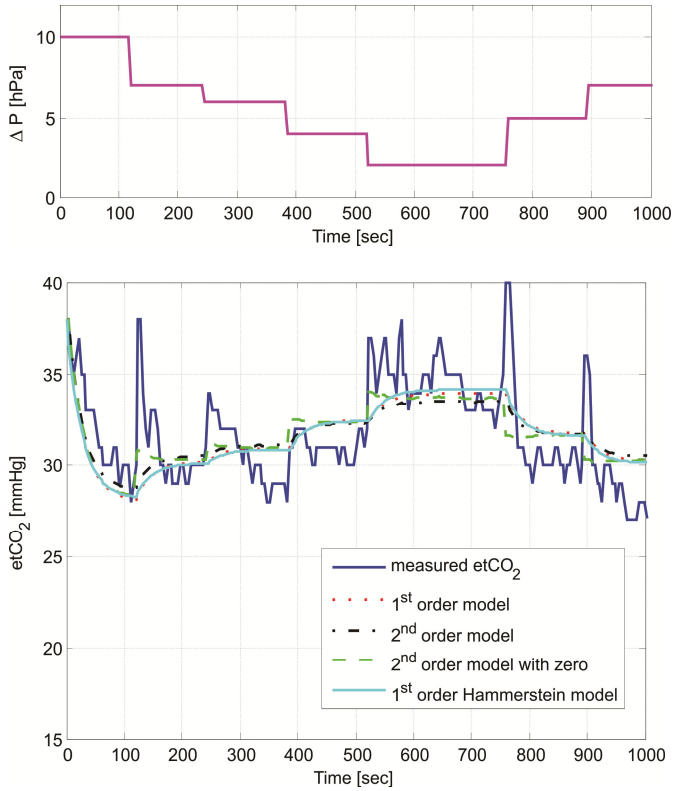

Fig. 4. Input-output measurements for system identification.

The model describing this system is identified using various model structures of both linear and non-linear models (Pottmann and Pearson, 1998). The results of parameter estimation are shown in Fig. 4, with a summary of performance results given in Table 1. The evaluation of different model structures is listed for 2 data sets, which are estimation and validation data. The mathematical forms of each particular model structure and the parameter estimation technique are provided in Appendix A. Based on a validation data set, a 1st order Hammerstein model gives the best result among all listed models. The 1st order linear model also offers the best RMS error among all linear models. Controller design and simulation are conducted with the 1st order linear model for the whole range of nonlinear operation in the following sections.

Table 1. Evaluation of model structure

	RMS error from estimation data	RMS error from validation set
1st order model	2.2475	2.2880
2nd order model	2.2116	2.2988
2nd order with one zero	2.1597	2.4093
1st order Hammerstein	2.1988	1.6709
2nd order Hammerstein	2.1680	1.7804
2nd order Hammerstein with one zero	2.1351	1.8085

Concerning the capnography for $etCO_2$ measurement, its accuracy is ±2 mmHg within the range for 0 - 40 mmHg, 5% of the reading for 41 - 70 mmHg and 8% of the reading for 71 - 150 mmHg. Considering this, the results of parameter estimation are in an acceptable range for the description of this system.

4. PROBLEM STATEMENT

The system to be controlled can be described as a SISO system.

$$y(s) = A(s)(u(s) + d(s)) \tag{2}$$

,where $y(s)$ is the Laplace transform of the measured $etCO_2$, $A(s)$ represents a strictly proper transfer function, $u(s)$ is the Laplace transform of the control input or ΔP in this system and $d(s)$ is the Laplace transform of the time-varying nonlinear uncertainties and disturbances $d(t)$ and generally assumed that $d(t) = f(t, y(t))$, where $f(t, y(t))$ satisfies Lipschitz continuity expressed in eq. (3) with Lipschtiz constant $L > 0$ and $L_0 > 0$.

$$\left|f(t, y_1) - f(t, y_2)\right| \le L\left|y_1 - y_2\right|, \ \left|f(t, y)\right| \le L\left|y\right| + L_0 \tag{3}$$

The control objective is to design a low frequency adaptive controller $u(t)$ using output feedback in a way that the system output $y(t)$ tracks the given reference input $r(t)$. Using a first-order reference model $M(s) = \frac{m}{s+m}$ for $m > 0$, the output provided in eq. (4) can be estimated by a multiplication between reference model and the reference signal.

$$y(s) \approx M(s)r(s) \tag{4}$$

Rewriting eq. (4) with the aid of eq. (2), we obtain

$$y(s) = M(s)(u(s) + \sigma(s)) \tag{5}$$

,where $\sigma(s) = \dfrac{A(s)u(s) + A(s)d(s) - M(s)u(s)}{M(s)}$.

Subsequently, the closed-loop adaptive control system can be formed based on the model reference $M(s)$.

5. L_1 ADAPTIVE CONTROLLER

The L_1 adaptive controller comprises 3 main components, namely an output predictor, an adaptive algorithm and a low-pass filter. Its performance is expected to be accurate, adaptive and robust for the control of $etCO_2$ in a wide range of ΔP inputs. The closed-loop structure of the L_1 adaptive control scheme is presented in Fig. 5.

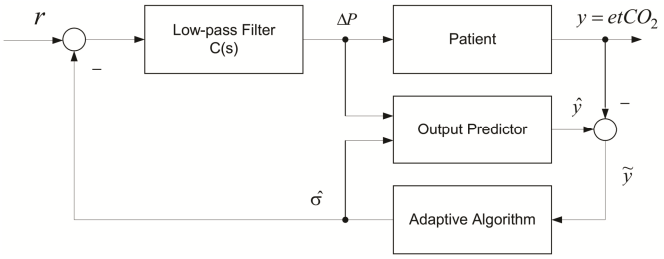

Fig. 5. Patient-in-the-loop configuration with L_1 adaptive controller.

Output predictor: The output predictor is designed to observe the predicted output $\hat{y}(t)$ with an adaptive mechanism from $\hat{\sigma}(t)$, where $\hat{\sigma}(t)$ is the adaptive estimator.

$$\dot{\hat{y}}(t) = -my(t) + m(u(t) + \hat{\sigma}(t)),\ \hat{y}(0) = 0 \tag{6}$$

Eq. 6 corresponds to the desired stable model reference system $M(s)$, which is designed using a first order differential equation.

Adaptive algorithm: The adaptive algorithm is used to adapt the reference signal for eliminating the output error and is defined by

$$\dot{\hat{\sigma}}(t) = \Gamma \cdot \Pr oj(\hat{\sigma}(t),\ -mP\tilde{y}(t)),\ \hat{\sigma}(0) = 0 \tag{7}$$

where $\Gamma \in R^+$ is the adaptation gain corresponding to the lower bound $\Gamma > \max\left\{\dfrac{\alpha\beta_3^2}{(\alpha-1)^2\beta_4 P}, \dfrac{\alpha\beta_4}{P\bar{\gamma}_0^2}\right\}$ with $\alpha > 1$ (Hovakimyan and Cao, 2010), $\Pr oj$ denotes the projection operator, which ensures that the signal $\hat{\sigma}(t)$ is restricted in a compact convex set with a smooth boundary (Cao and Hovakimyan, 2007a), $\tilde{y}(t) = \hat{y}(t) - y(t)$, and P is obtained by solving the well-known Lyapunov equation.

A low-pass filter is introduced to eliminate high frequency components in the control signal. An abrupt change of the pressure difference will be avoided by this filter. The control law is computed by eq. (8).

$$u(s) = C(s)(r(s) - \hat{\sigma}(s)) \tag{8}$$

where $C(s) = \dfrac{\omega}{s+\omega}$ and is subject to the L_1 gain stability requirement (Cao and Hovakimyan, 2007a). Therefore, our choices to design $M(s)$ and $C(s)$ are limited by

$$H(s) = \frac{A(s)M(s)}{C(s)A(s) + (1 - C(s))M(s)} \tag{9}$$

is stable and

$$\left\|G(s)\right\|_{L_1} L < 1 \tag{10}$$

where $G(s) = H(s)(1 - C(s))$.

The proof (Hovayakim *et al.*, 2011) shows that the error norm is inversely proportional to the square root of the adaptation gain. Therefore, the design of high adaptation gain Γ will minimize the error norm $\tilde{y}(t)$. A high Γ will be used in design of our control system. However, it is not possible to introduce an extremely high adaptation gain because of the computational limitation of the processor being used for the controller.

6. SIMULATION RESULTS AND DISCUSSION

The models from system identification obtained from section 3 are analyzed for the control system design using linear and Hammerstein models. A limitation of ΔP between 2 and 40 hPa is introduced for safety reasons. The parameters of the L_1 adaptive controller are designed by $\Gamma = 40000$ and different low-pass filters at $\omega = 0.03$, 0.05 and 0.1 rad/sec are evaluated in our study. The desired $etCO_2$ is set at 35 mmHg and the results of the control signal ΔP and the output signal $etCO_2$ are shown in Fig. 6.

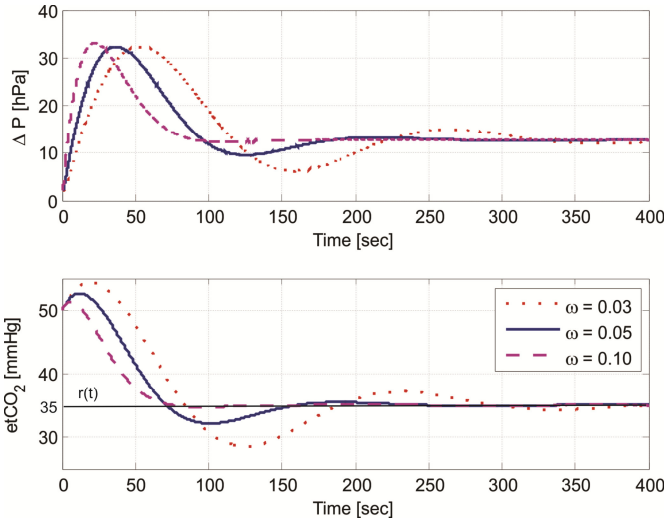

Fig. 6. Simulation results of control input and $etCO_2$ output based on a 1st order linear model with different cut-off frequencies of the low-pass filter.

The higher the bandwidth of the low-pass filter, the faster the response. The bandwidth at $\omega = 0.10$ rad/sec provides us the settling time of 90 sec with no steady state error. There is no chattering effect on the control channel for all of the selected bandwidths in the simulation. Furthermore, Gaussian white noise with a standard deviation of 1 mmHg was introduced into the system to observe the control performance and disturbance rejection of the L_1 adaptive controller. Further investigation are carried out based on disturbances with different power and in various conditions of pole uncertainty. The simulation results are shown in Fig. 7. The L_1 adaptive controller shows good robustness at disturbance power up to 1.5 $mmHg^2sec/rad$. The control can tolerate a pole uncertainty between -28% and 23%. If the uncertainty beyond this range is introduced, loss of control can occur.

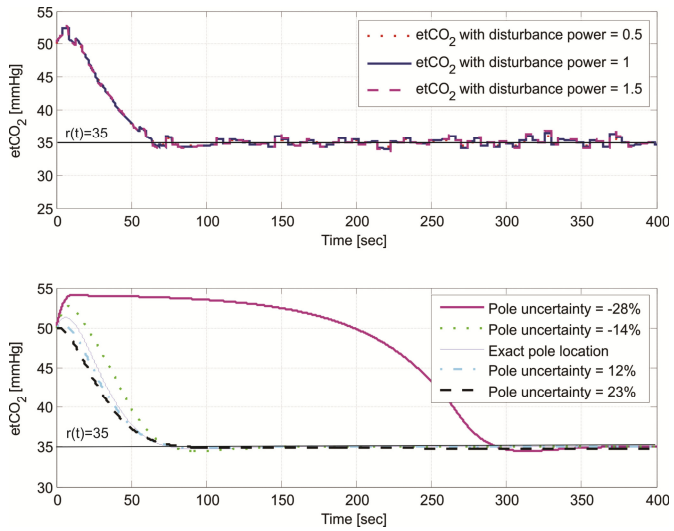

Fig. 7. Simulated output response of $etCO_2$ with disturbance and pole uncertainty using a 1st order linear process model.

When the pole moves further into the left-half plane (pole uncertainty changes from -28% to 23%), a faster output response of $etCO_2$ can be observed by a shorter settling time with no steady state error. The success or failure of this controller relies mainly on pole uncertainty of the output predictor.

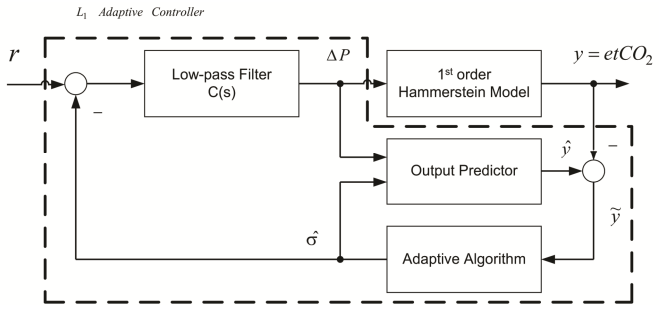

Fig. 8. Block diagram for the simulation using a 1st order Hammerstein model as a plant with the designed L_1 adaptive controller using a 1st order linear model.

Further investigation is carried out with a 1st order Hammerstein plant based on the designed parameters using a first order linear model for the design of the L_1 adaptive controller. The structure of this simulation is presented in Fig. 8. It closely imitates the real application of this controller for the nonlinear time-varying plant or the mechanically ventilated patient. However, in some cases, a loss of control in $etCO_2$ can be observed in the simulation. The control signal ΔP is delivered at the maximum of the saturated safety range and it holds the unsatisfying value for a longer duration. Therefore, a retuning is necessary if we apply the L_1 adaptive controller under these realistic situation. Thus, the initial condition of $\hat{\sigma}$ in the projection of the adaptive algorithm is adjusted as well as the cut-off frequency of the low-pass filter is reduced. The simulation result with additive Gaussian white noise of power 0.5 is shown in Fig. 9. The desired reference $r(t)$ is set at 35 mmHg at the simulation time $t < 200$ sec and a step is introduced at 40 mmHg at $t \geq 200$ sec.

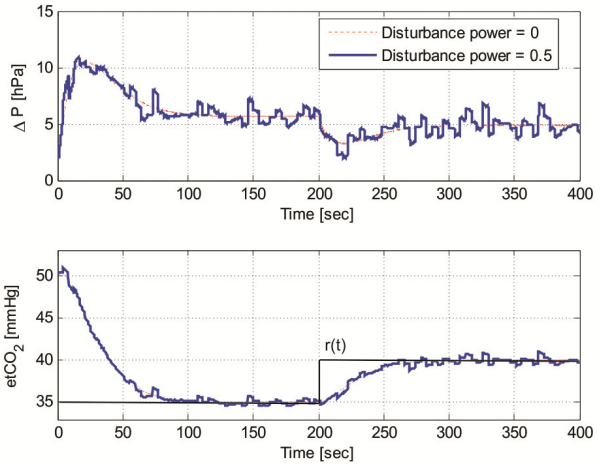

Fig. 9. Simulation result for the tracking performance of L_1 adaptive controller for a nonlinear Hammerstein model with $r(t) = 35$ mmHg for $t < 200$ sec and $r(t) = 40$ mmHg for $t \geq 200$ sec.

Fig. 9 shows that the $etCO_2$ response reaches the desired reference signal approximately 100 sec after the step change. The pole of the model is located in the left half plane close to the origin of the complex plane at -0.0334 and the response is relatively slow but acceptable for the cardiopulmonary system. Concerning the control signal ΔP, the overshoot is also in an acceptable range for implementation. The controller can successfully tolerate the disturbance introduced into the system. The L_1 adaptive controller can be considered as a promising solution for the control of $etCO_2$ for the nonlinear time-varying plant. However, the disturbance may cause a fast change of ΔP and result in a frequent change in tidal volume. To test this controller with the patient, a fine tuning might be necessary during the experiment.

In the future, a more generalized approach should be introduced for the model formulation of different PEEP values. The model should describe patients with various physiological properties (large vs. small, sick lung vs. healthy) and with different PEEP setting. Basically, the PEEP

parameter influences functional residual capacity (FRC). More PEEP will definitely give a larger lung volume at the end of expiration and it causes a change in $etCO_2$. In this study, a simplification is made for a fixed PEEP at 5 hPa. Secondly, it should be noted that our control method can be applied for inhomogeneous lung model e.g. a lung with a restrictive disease (Acute Respiratory Distress Syndrome - ARDS). But it may cause overdistension of aerated alveoli and volutrauma, just targeting $etCO_2$ and not minimizing shear stress in the alveoli. Also, the control of $etCO_2$ in diseased lungs has an even more complicated relationship to the physiological target value of $PaCO_2$ in blood, which depends on individuality and the severity of the disease.

7. CONCLUSION

This article presents the design of L_1 adaptive controller to control $etCO_2$ for a patient undergoing mechanical ventilation with a homogeneous lung model. Using pressure-controlled ventilation, a patient model from a male volunteer is identified using linear and nonlinear Hammerstein models. Based on the obtained models, the tracking performance and robustness of the controller are evaluated by a simulation with dynamic disturbance injection and pole uncertainty. The nonlinear Hammerstein extension is made for the feasibility study of real clinical implementation. The controller showed stability and good performance in terms of adaptation to the uncertain, perturbed system, thus good results in the clinical application scenario can be expected. The L_1 adaptive controller provides a practical solution for the control of $etCO_2$ to deal with the nonlinear time-varying system and as a secondary effect optimizes the muscular power of the respiratory system as well.

ACKNOWLEDGEMENTS

The authors acknowledge the financial support of German Federal Ministry of Science and Education (BMBF) through the OXIvent project under the grant 16SV5605.

REFERENCES

Benallal, H., and Busso, T. (2000). Analysis of end-tidal and arterial PCO_2 gradients using a breathing model. *Eur J Appl Physiol*, volume (83), 402-408.

Cao, C., and Havakimyan, N. (2007a). L_1 adaptive output feedback controller for systems with time-varying unknown parameters and bounded disturbances. *Proceedings of the 2007 American Control Conference*, 486-491.

Cao, C., and Havakimyan, N. (2007b). L_1 adaptive output feedback controller to systems of unknown dimension. *Proceedings of the 2007 American Control Conference*, 1191-1196.

Cao, C., and Havakimyan, N. (2006). Design and analysis of a novel L1 adaptive controller, Part I: Control signal and asymptotic stability. Proceedings of the 2006 American Control Conference, 3397-3402.

Feng, G., and Lozano, R. (1999). Adaptive control systems. Reed Educational and Professional Publishing Ltd, Oxford, UK.

Gregory, I.M., Cao, C., Xargay, E., Hovakimyan, N., and Zou, X. (2009). L_1 adaptive control design for NASA AirSTAR flight test vehicle**,** *AIAA Guidance, Navigation, and Control Conference*, 2009-5738.

Hovakimyan, N. and Cao, C. (2010). L_1 adaptive control theory. SIAM Society for Industrial and Applied Mathematics, Philadelphia, USA.

Hovakimyan, N., Cao, C., Kharisov E., Xargay E., and Gregory I.M. (2011). L_1 adaptive control for safety-critical systems. *IEEE Contr. Syst. Mag.*, volume (31), 54-104.

Kharisov, E., Beck, C.L., and Bloom, M. (2011). Control of patient response to anesthesia using L_1 adaptive methods, *8th IFAC Symposium on Biomedical and Medical Systems*, volume (8), 391-396.

Pomprapa, A (2013). System Identification and Robust Control Design for End-tidal CO_2 using H-infinity Loop-shaping. *17th International Student Conference on Electrical Engineering POSTER 2013 in Prague*, BI14.

Pottmann, M. and Pearson, R. K. (1998). Block-oriented NARMAX models with output multiplicities. *AIChE Journal*, volume (44), 131-140.

Ralph, M., Beck, C.L. and Bloom, M. (2011). L_1-adaptive methods for control of patient response to anesthesia. *American Control Conference*, 1729-1735.

Stroosma, O., Damveld, H.M., Mulder, J.A., Choe, R., Xargay, E., and Hovakimyan, N. (2011). A handling qualities assessment of a business jet augmented with an L_1 adaptive controller, *AIAA Guidance, Navigation, and Control Conference*, AIAA 2011-6610.

Tan, Y., Moase W.H., Manzie C., Nesic D., Mareels, I.M.Y. (2010). Extremum seeking from 1922 to 2010. *Proceedings of the 29th Chinese Control Conference*, 14-26.

Appendix A. MODEL STRUCTURE

The model structures in this paper are given in this section for a 1st order linear model, 2nd order linear model, 2nd order linear model with zero, 1st order Hammerstein model, 2nd order Hammerstein model and 2nd order Hammerstein model with zero as stated in (11) - (16), respectively. The model parameters can be estimated from data by a least squares algorithm.

$$\dot{y}(t) = ay(t) + bu(t) \tag{11}$$

$$\ddot{y}(t) = a_1\dot{y}(t) + a_2 y(t) + bu(t) \tag{12}$$

$$\dddot{y}(t) = a_1\dot{y}(t) + a_2 y(t) + b_1\dot{u}(t) + b_2 u(t) \tag{13}$$

$$\dot{y}(t) = ay(t) + bN[u(t)] \tag{14}$$

$$\ddot{y}(t) = a_1\dot{y}(t) + a_2 y(t) + bN[u(t)] \tag{15}$$

$$\ddot{y}(t) = a_1\dot{y}(t) + a_2 y(t) + b_1 N[\dot{u}(t)] + b_2 N[u(t)] \tag{16}$$